



Confined Water in Mesoporous MCM-41 and Nanoporous $\text{AlPO}_4\text{-5}$: Structure and Dynamics

NICOLE FLOQUET* AND JEAN PAUL COULOMB

C.R.M.C.N - CNRS, Campus de Luminy, Case 901, 13288 Marseille Cedex 9, France

floquet@crmcn.univ-mrs.fr

NATHALIE DUFAU

MADIREL - UMR 6121, Centre de St Jérôme, 13397 Marseille Cedex 20, France

GILLES ANDRE AND REMI KAHN

Laboratoire Léon - Brillouin, CEA - Saclay, 91191 Gif - sur - Yvette, Saclay, France

Abstract. Confined water presents unusual properties in comparison with other sorbate species. First of all, the sorption isotherm is of type III, even in the microporous confinement range ($\emptyset < 20 \text{ \AA}$). Whatever the pore diameter, water sorption phenomenon looks like the so-called capillary condensation phase transition. Our results clearly valid such an expected behaviour in the mesoporous confinement range ($20 \text{ \AA} < \emptyset < 40 \text{ \AA}$). The water confined phase is a liquid phase characterized by a short range order and a high translational molecular mobility. The confinement induces a strong displacement towards the low temperature of the water confined liquid solidification T_{sol} . (for instance, $T_{\text{sol}} = 230 \text{ K}$ for D_2O confined liquid in MCM-41 ($\emptyset = 24 \text{ \AA}$). We have determined the structure of the water confined solid phase observed below T_{sol} . It looks like those of the cubic ice structure affected by strong quasi-isotropic finite size effects induced by the confinement. Such a quasi-(1d) solid appears as a polycrystalline column rather than a single crystalline nanofiber. Concerning water confinement in the microporous range (as for example, $\text{AlPO}_4\text{-5}$ zeolite ($\emptyset = 7.3 \text{ \AA}$)), our results are more surprising. Type III sorption isotherm is the signature of a crystallization phenomenon at room temperature ($T = 300 \text{ K}$). The confined water crystallizes in two helices that are commensurate with the $\text{AlPO}_4\text{-5}$ micropore structure. The confined ice has a density of $1.2 \text{ g}\cdot\text{cm}^{-3}$.

Keywords: confinement, water, MCM-41, $\text{AlPO}_4\text{-5}$, neutron scattering

1. Introduction

Due to its major importance in several scientific domains (biology, geology, climatology), the different water properties have been intensively investigated. A lot of papers are for instance devoted to the rich and complex water phase diagram (at least two amorphous solids and twelve different ices). Consequently, the confined water properties have been investigated years ago. A large number of natural or synthetic porous ma-

terials were used as sorbant samples (clays, coals, zeolites, different porous glasses). Among the more recent researches, numerous studies concern water confined phase in porous vycor glass, for example, those from Dunn et al. (1988), Bellisent-Funel et al. (1993) and Dore (2000). Interesting results were obtained, and for instance, those concerning the water triple point depression. But, the large pore size distribution and the pore connectivity which characterize vycor glass samples, might blur some observations.

In the mesoporous confinement range, MCM-41 host material is much more suited for detailed analysis of

*To whom correspondence should be addressed.

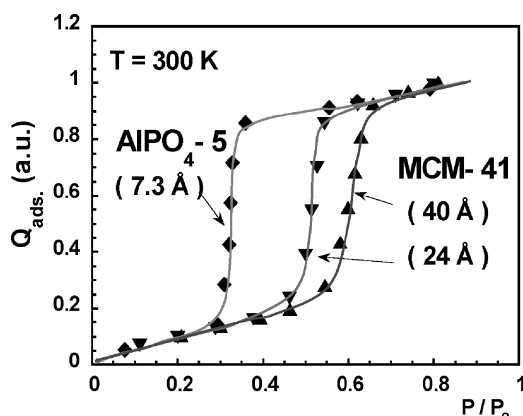


Figure 1. Water sorption isotherms measured at $T = 300$ K for an $\text{AlPO}_4\text{-5}$ zeolite sample ($\varnothing = 7.3$ Å) and for two MCM-41 samples characterized by a pore diameter \varnothing equal to 24 Å and 40 Å respectively. The loadings have been normalized to the loading maximum (arbitrarily located at $p/p_0 = 0.8$) to help the comparison.

the confined water properties. Morishige's research group seems to share our point of view (Morishige et al., 1997). Generally speaking, the adsorbed species in MCM-41 samples are characterized by type IV sorption isotherms. But, as shown in Fig. 1, water sorption isotherm in MCM-41 samples is of type III. For methane or deuterium, the capillary condensation arises after a physisorbed film formation. Concerning water sorbate, such a film does not grow, only the capillary condensation phenomenon is observed. Water does not wet the MCM-41 inner surface. The quasi vertical step (which is the capillary condensation signature) moves down to the low relative pressure (p/p_0) side when decreasing the pore diameter. The hysteresis loop of H1 type is also generally well observed.

In the microporous range, as in zeolites, sorbate confinement could have unexpected signature. Thus, the water sorption isotherm in $\text{AlPO}_4\text{-5}$ zeolite ($\varnothing = 7.3$ Å) belongs to the type III isotherm as in MCM-41 material as highlighted in the Fig. 1. Recall that the usual sorption isotherm type in zeolites is of type I (as shown in Fig. 2, for instance for the methane or deuterium sorbates in $\text{AlPO}_4\text{-5}$). This originality of water sorption in $\text{AlPO}_4\text{-5}$ is prominent when compared with sorption isotherms of other sorbate species. Moreover there is an exceptionally large water sorption capacity of $\text{AlPO}_4\text{-5}$ in comparison with that of a smaller molecule such as deuterium. It is also interesting to compare the sorption of the same molecular species

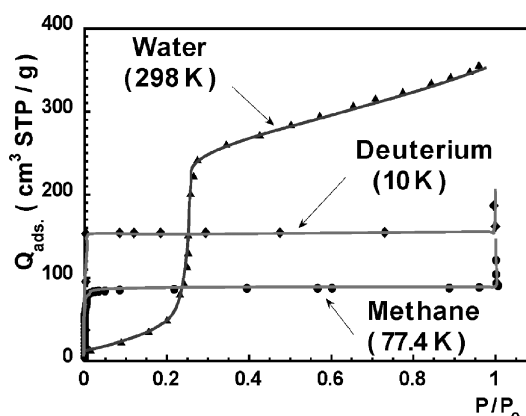


Figure 2. Sorption isotherms of water (type III) methane (type I) and deuterium (type I), measured at $T = 298$ K, $T = 77.4$ K and $T = 110$ K respectively in $\text{AlPO}_4\text{-5}$ zeolite sample ($\varnothing = 7.3$ Å).

in MCM-41 and in $\text{AlPO}_4\text{-5}$. Such results have been already published in the literature by several groups (Lohse et al., 1986; Choudhary et al., 1988; Malla et al., 1995; Izmailova et al., 1996; Kolesnikov et al., 1997; Tsutsumi et al., 1999). It is merely interpreted as an extra sorption in the secondary small hexagonal micropores of the $\text{AlPO}_4\text{-5}$ framework porosity (Davis et al., 1989; Newalkar et al., 1998). One motivation of our investigations was to valid or not such a conjecture. But the aim of the present paper is to outline the structural and dynamic properties of water phases confined in these both types of porous materials: MCM-41 and $\text{AlPO}_4\text{-5}$.

2. Experimental Section

The $\text{AlPO}_4\text{-5}$ zeolite sample and the MCM-41 ($\varnothing = 19$ and 24 Å) sample used in the present experiments were synthesized at the Laboratoire des Matériaux Minéraux (Mulhouse–France). Concerning the MCM-41 ($\varnothing = 25$ Å) and ($\varnothing = 40$ Å) samples, they were prepared at the Laboratory of Inorganic Chemistry (Mainz–RFA). Prior to any experiments (calibration isotherms or neutron scattering measurements), the samples are out-gassed under vacuum ($P \leq 10^{-6}$ Torr) over a night at $T > 250^\circ\text{C}$. Neutron scattering experiments were performed at the Laboratoire Léon–Brillouin (C.E.N.–Saclay). For neutron diffraction and incoherent quasi-elastic neutron scattering measurements, the two axis diffractometer G4-1 and the time of flight MIBEMOL were used respectively.

3. Results and Discussion

Both the structural and dynamic properties of confined water in several MCM-41 samples (19, 24 and 40 Å) and in AlPO₄-5 zeolite were investigated by neutron scattering.

3.1. Water Sorption in the Mesopores of the MCM-41 Samples

Some results have been already published, they concern MCM-41 samples overloaded with water (D₂O) (Floquet et al., 1999; Coulomb et al., 2000). Thus, in these previous reports, the confined water in the host porous material was coexisting with bulk (3d) water located on the external MCM-41 surface. In the present study, the relative water vapor pressure p/p_0 was monitored to be always smaller than one ($p/p_0 < 1$) to prevent any bulk water formation. The detailed structural analysis concerns the confined heavy water in MCM-41 ($\varnothing = 24$ Å). The measured diffractograms at almost full loading (loading = 95%) for different temperatures in the range 173–280 K are represented in Fig. 3.

The measured diffractogram characteristics are temperature dependent. At high temperature, $T = 280$ K, the confined water neutron diffraction signal appears as a wide bump located at around $Q = 1.85$ Å⁻¹. Whereas, at low temperature, $T = 173$ K, the signal looks much more like to a diffraction peak (which is now located at smaller wave vector ($Q \approx 1.7$ Å⁻¹)). Clearly something happens in the temperature range 219–239 K, the solidification of the confined water

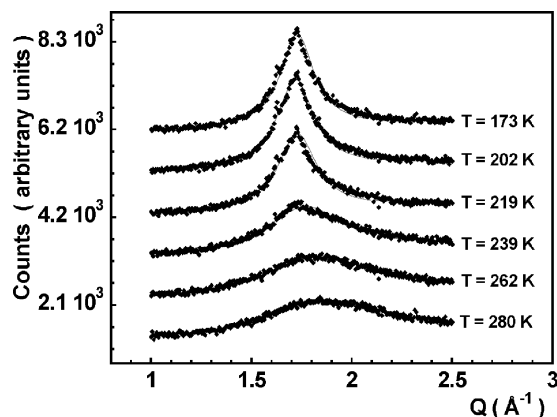


Figure 3. Measured neutron diffractograms of confined water D₂O sorbed in MCM-41 sample ($\varnothing = 24$ Å) at almost full loading (95%) for different temperatures in the range 173–280 K.

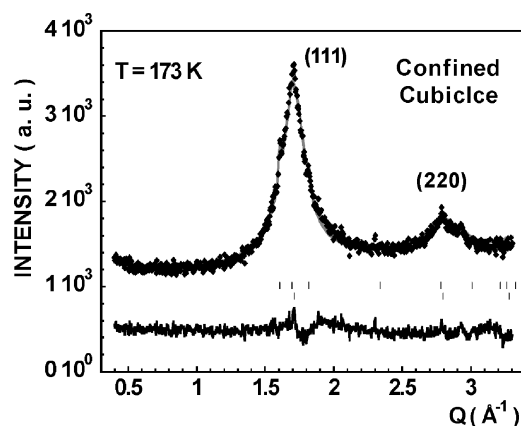


Figure 4. Cubic ice structure of the confined solid phase of water D₂O sorbed at $T = 173$ K in MCM-41 sample ($\varnothing = 24$ Å) at almost full loading (95%). Strong finite size effects are observed due to the confinement in MCM-41 mesopores.

phase was conjectured. The determination of the structure of the confined water solid phase was attempted from the low temperature measured diffractograms. Both the bulk hexagonal ice structure and the bulk cubic ice structure were considered. Our basic simple idea is that strong finite size effects must be induced by the MCM-41 pore confinement. Detailed relationships between finite size effects and diffractogram modifications were determined. Diffractograms were calculated with the powerful program of structure determination (FULLPROF elaborated by J. Rodriguez-Carvajal). The result of our best fit is given in Fig. 4, the measured diffractogram at $T = 173$ K, the calculated diffractogram from the cubic ice structure and their difference are represented (the fit reliability factor is acceptable $R = 10.5\%$). Only the two diffraction peaks ((111) and (220)) of the cubic ice structure are observed in our experimental wave vector range. Such diffraction peaks are strongly widened by isotropic finite size effects. An other attempt is to fit the experimental data with the bulk hexagonal ice structure, but the agreement is poor due to the absence of any (102) observed peak around $Q = 2.3$ Å⁻¹. This analysis suggests a cubic ice like structure for the water confined solid phase in MCM-41 sample. Note that tiny signature of narrow diffraction peak of the bulk hexagonal structure is observed. Presumably during the cooling down to $T = 173$ K, when the confined water phase freezes due to dilatation effect at the considered loading (loading = 95%), very small amount of confined ice is pushing outside the pore and is then freezing in its hexagonal structure.

The neutron diffractograms measured at higher temperatures were also fitted with the cubic ice structure of water (the coherence length was the main adjustable parameter used). Keeping in mind that our model is valid only for crystalline solid phase, the agreement with the experimental data is rather good. The quantitative determination of the coherence length L_{coher} versus temperature allowed a more precise determination of the melting temperature T_m of the confined cubic ice in MCM-41 ($\Phi = 24 \text{ \AA}$): $T_m = 228 \pm 2 \text{ K}$.

3.2. Water Sorption in the Micropores of the $\text{AlPO}_4\text{-5}$ Zeolite

Both the structural and the dynamic properties of the confined water in an ultra confinement regime were investigated by neutron scattering. Concerning the structural analysis, the neutron diffractograms of sorbed water were measured at $T = 300 \text{ K}$ in $\text{AlPO}_4\text{-5}$ zeolite for different loadings. The diffractograms are represented in Fig. 5. Strong modifications of the $\text{AlPO}_4\text{-5}$ empty zeolite diffractogram were observed upon water sorption. The more visible one is the constant intensity decrease of the main diffraction (100) peak. The intensity background is also modified. A very wide peak (not visible at the present scale) exists at high loading (Load. = 95%) in the wave vector range $Q = 1.5\text{--}3 \text{ \AA}^{-1}$ (see above Fig. 8). As it will be discussed below in the text, this broadened peak represents the confined water D_2O signal strongly widened by finite size effect. Before any attempt in confined water structure

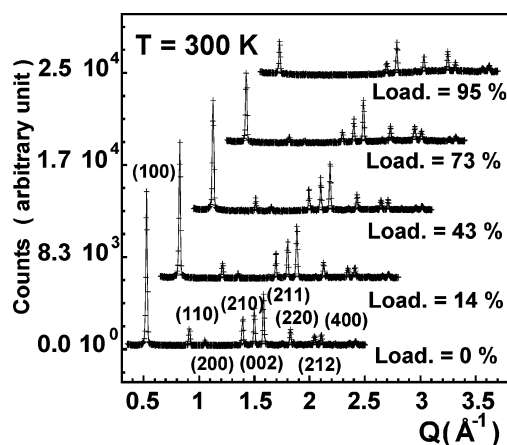


Figure 5. Measured neutron diffractograms of confined heavy water (D_2O) at $T = 300 \text{ K}$ in $\text{AlPO}_4\text{-5}$ zeolite for different loading (14, 43, 73 and 95%).

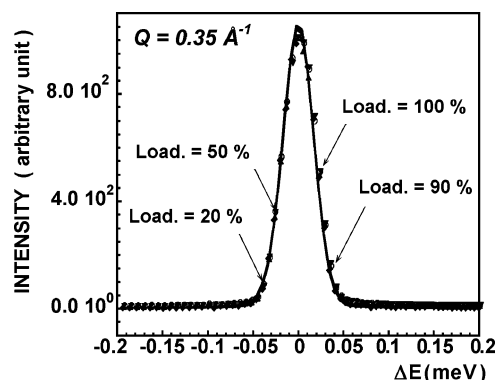


Figure 6. Measured incoherent quasi-elastic neutron scattering spectra of H_2O confined phase in $\text{AlPO}_4\text{-5}$ zeolite. The different water loading (20, 50, 90 and 100%) are deduced from the calibration isotherm. Intensity of the different spectra are normalised to an arbitrary value 10^3 .

characterizing, our first aim was to determine the influence of water sorption in the secondary hexagonal micropores of the $\text{AlPO}_4\text{-5}$ zeolite on the diffractogram characteristics. Our calculation clearly points out that the D_2O confinement in the secondary hexagonal pore of $\text{AlPO}_4\text{-5}$ strongly increases the (100) peak intensity, whereas its measured intensity decreases continuously. Consequently, the conjecture about an initial sorption of 4 molecules of water in the 6-membered hexagonal $\text{AlPO}_4\text{-5}$ micropores is wrong (Davis et al., 1989; Newalkar et al., 1998). The thorough analysis of the whole set of diffractograms recorded at different water loadings confirms that water molecules physisorb first on the inner surface of the $\text{AlPO}_4\text{-5}$ main pores (the 12-membered hexagonal pores). The capillary condensation step corresponds to the growth of water molecule chains characterized by a double helix morphology commensurate with the $\text{AlPO}_4\text{-5}$ main pores (Floquet et al., 2004). This very new finding adds to the originality of the properties of the confined water in $\text{AlPO}_4\text{-5}$ zeolite.

Our study by incoherent quasi-elastic neutron scattering (IQNS) of the $\text{H}_2\text{O}/\text{AlPO}_4\text{-5}$ system brings additional information about this confined water phase. Thus, there is no difference in the calibration isotherms measured at $T = 300 \text{ K}$ due to isotopic effects between H_2O and D_2O . The IQNS signal is proportional to the confined water loading. Figure 7 gives the IQNS spectra measured for different H_2O loadings and normalised to the arbitrary 10^3 intensity value. There is no quasi-elastic broadening of the signal at the different loading, the IQNS signal is a pure elastic line similar

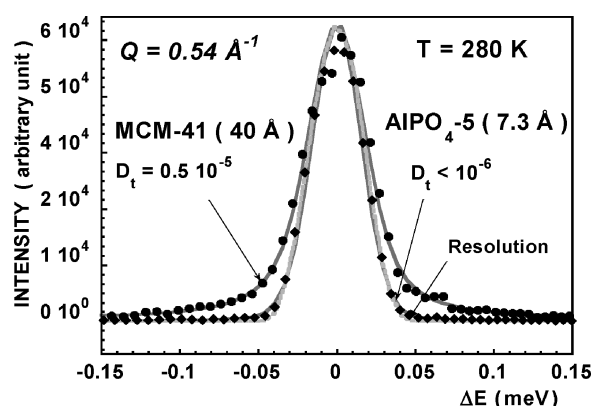


Figure 7. Measured IQNS spectra of confined water at $T = 280$ K for a loading equal to (Load = 90%) in AlPO₄-5 zeolite and MCM-41 ($\varnothing = 40$ Å) sample.

to the instrumental resolution. It is deduced that, at $T = 300$ K, the water molecular translational mobility D_t is quite small $D_t < 10^{-6}$ cm² s⁻¹. This result confirms that the confined water phase in AlPO₄-5 micropore is an icy like phase. The commensurability of the water solid chain with the AlPO₄-5 inner surface periodicity should explain its stability at room temperature. Recall that for (2d) phases, any commensurability effect displaces the melting temperature to the high temperature side.

3.3. Confined Water Properties in the Mesoporous and Microporous Confinement Range

Clear illustration of the IQNS spectra differences between water confined at $T = 280$ K in MCM-41 ($\varnothing = 40$ Å) sample and in AlPO₄-5 zeolite sample, are shown in Fig. 7. Large quasi-elastic peak broadening corresponding to a water molecular translational mobility D_t ($D_t = 0.5 \cdot 10^{-5}$ cm² s⁻¹) is observed for the H₂O/MCM-41 ($\varnothing = 40$ Å) system. The IQNS signal of water confined in AlPO₄-5 zeolite is quite the same than the instrumental resolution ($D_t < 10^{-6}$ cm² s⁻¹). The nature of the confined water phases is different in the room temperature range (280–300 K) between MCM-41 samples (confined liquid state) and AlPO₄-5 zeolite (confined solid state).

For ultra confinement of solid phase, such as described in the case of H₂O/MCM-41, the finite size effects are so strong that they induce large diffraction peak broadening which looks like short range order signature. Figure 8 gives a good illustration of short

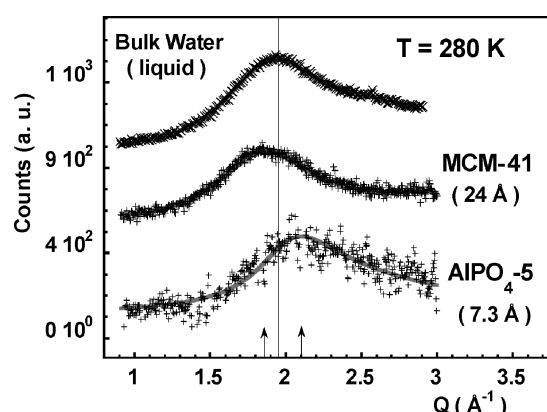


Figure 8. Measured neutron diffractograms at $T = 280$ K of bulk (3d) liquid water and confined water in MCM-41 ($\varnothing = 24$ Å) and AlPO₄-5 zeolite ($\varnothing = 7.3$ Å) at loading equal to 95%.

range order which characterizes both the bulk (3d) water liquid phase and the confined water liquid phase in MCM-41 ($\varnothing = 24$ Å) in comparison with the large finite size effects which affect the water solid chain confined in AlPO₄-5 zeolite. Thus, due to confinement effects, neutron diffraction signals of the confined phase do not allow to determine the confined water state (liquid or solid confined phase), but the IQNS analysis does.

4. Conclusion

Our results point out the original properties of confined water in model host materials such as MCM-41 samples and AlPO₄-5 zeolite. In the medium confinement regime, as for water/MCM-41 systems, usual molecular water organisation is observed (confined liquid phase, confined cubic ice phase). The confinement effect is the displacement of the whole water phase diagram towards the low temperature side (decreasing the MCM-41 pore size increases the temperature displacement). In the ultra confinement range, in addition to confinement effect, there is a large influence of the host material walls. Our finding is a new molecular water organisation characterized by a high density (around 1.2 g.cm⁻³) and a double helix morphology which is stable at room temperature $T = 300$ K. The determination of its temperature range stability is in progress. Concerning the surprising large density of the quasi-(1d) ice like phase, it might result from several additive factors, as for instance, the AlPO₄-5 wall potential influence (which acts like an external pressure), the hydrogen

bonds formation between confined water and the oxygen atoms of the zeolite inner surface, commensurability effects between such new ice type and the sorption sites of the $\text{AlPO}_4\text{-5}$ inner surface.

References

- Belliscent-Funel, M.-C., J. Lal, and L. Bosio, "Structural Study of Water Confined in Porous Glass by Neutron Scattering," *J. Chem. Phys.*, **98**, 4246–4252 (1993).
- Choudhary, V.R., D.B. Akolekar, A.P. Singh, and S.D. Sansare, "Influence of Thermal, Hydrothermal, and Acid-Base Treatments on Structural Stability and Surface and Catalytic Properties of $\text{AlPO}_4\text{-5}$," *J. Catal.*, **111**, 253–263 (1988).
- Coulomb, J.P., N. Floquet, Y. Grillet, P.L. Llewellyn, R. Kahn, and G. André, "Dynamic and Structural Properties of Confined Phases (Hydrogen, Methane and Water) in MCM-41 samples (1.9 nm, 2.5 nm and 4 nm)," *Studies in Surface Science and Catalysis*, **128**, 235–242 (2000).
- Davis, M.E., C. Montes, P.E. Hathaway, J.P. Arhancet, D.L. Hasta, and J.M. Garces, "Physicochemical Properties of VP 1-5," *J. Am. Chem. Soc.*, **111**, 3919–3927 (1989).
- Dore, J.C., "Structural Studies of Water in Confined Geometry by Neutron Diffraction," *Chem. Phys.*, **258**, 327–347 (2000).
- Dunn, M., J.C. Dore, and P. Chieux, "Structural Studies of Ice Formation in Porous Silicas by Neutron Diffraction," *J. Cryst. Growth*, **92**, 233–238 (1988).
- Floquet, N., J.P. Coulomb, N. Dufau, and G. André, "Structural and Dynamics of Confined Water in $\text{AlPO}_4\text{-5}$ Zeolite," *J. Phys. Chem. B.*, **108** 13107–13115 (2004).
- Floquet, N., J.P. Coulomb, N. Dufau, G. André, and R. Kahn, "Structural and Dynamic Properties of Confined Water in Nanometric Model Porous Materials ($8 \text{ \AA} \leq \varnothing \leq 40 \text{ \AA}$)," *Physica B*, **350**, 265–269 (2004).
- Floquet, N., J.P. Coulomb, C. Martin, Y. Grillet, P.L. Llewellyn, and G. André, "Neutron Diffraction Study of Phase Transitions observed during the Sorption of D_2O on MCM-41 (40 \AA and 25 \AA)," in *Proceedings of the 12th Int. Zeolite conference*, M.J. Treacy et al., pp. 659–666, Material Research Society, 1999.
- Izmailova, S.G., E.A. Vasiljeva, I.V. Karetina, N.N. Feoktistova, and S.S. Khvoshchev, "Adsorption of Methanol, Ammonia and Water on the Zeolite-Like Aluminophosphates $\text{AlPO}_4\text{-5}$, $\text{AlPO}_4\text{-17}$, and $\text{AlPO}_4\text{-18}$," *J. Colloid Interface Sci.*, **179**, 374–379 (1996).
- Kolesnikov, A.I., V.V. Sinitsyn, E.G. Ponyatovsky, I. Natkaniec, L.S. Smirnov, and J.C. Li, "Neutron-Scattering Studies of Ice Prepared by Different Thermobaric Treatments," *J. Phys. Chem.*, **101**, 6082–6086 (1997).
- Lohse, J., M. Noack, and E. Jahn, "Adsorption Properties of the $\text{AlPO}_4\text{-5}$ Molecular Sieve," *Adsorption Science and Technology*, **3**, 19–24 (1986).
- Malla, P.B. and S. Komarneni, "Effect of Pore Size on the Chemical Removal of Organic Template Molecules from Synthetic Molecular Sieves," *Zeolite*, **15**, 324–332 (1995).
- Morishige, K. and K. Nobuoka, "X-ray Diffraction Studies of Freezing and Melting of Water Confined in a Mesoporous Adsorbent (MCM-41)," *J. Chem. Phys.*, **107**, 6965–6969 (1997).
- Newalkar, B.L., R.V. Jasra, V. Kamath, and S.G.T. Bhat, "Sorption of Water in Aluminophosphate Molecular Sieve $\text{AlPO}_4\text{-5}$," *Micropor. Mesopor. Mater.*, **20**, 129–137 (1998).
- Tsutsumi, K., K. Mizoe, and K. Chubachi, "Adsorption Characteristics and Surface Free Energy of $\text{AlPO}_4\text{-5}$," *Colloid Polym. Sci.*, **277**, 83–88 (1999).